Nuclear Mathematical and Computational Sciences: A Century in Review, A Century Anew
Gatlinburg, Tennessee, April 6-11, 2003, on CD-ROM, American Nuclear Society, LaGrange Park, IL (2003)

DIFFUSION-LIKE 3-D HETEROGENEOUS CORE CALCULATION WITH 2-D CHARACTERISTICS TRANSPORT CORRECTION BY NON-LINEAR ITERATION TECHNIQUE

Shinya Kosaka
Tepco Systems Corporation
Tokyo Bijyutsu Club Bldg., 6-19-15 Shimbashi, Minato-ku
105-0004 Tokyo, Japan
kosaka-shinya@tepsys.co.jp

Toshikazu Takeda
Osaka University
Yamadaoka, Suita-shi, 565-0871 Osaka, Japan
takeda@nucl.eng.osaka-u.ac.jp

ABSTRACT

A method for diffusion-like 3-D heterogeneous core calculations, which is corrected by the method of characteristics(MOC) 2-D solutions horizontally and solved by the diffusion theory axially, is demonstrated and verified its applications in this paper.
In this method, 2-D MOC corrected 3-D heterogeneous core calculation is achieved by utilizing the non-linear iteration technique which is commonly used in advanced nodal diffusion codes. To take account of the heterogeneous transport effects in the horizontal direction, the additional diffusion-like coefficients used in the non-linear iteration are obtained from the results of 2-D MOC heterogeneous fixed-source calculations at each horizontal plane. The usual diffusion theory is applied for the axial direction, so far. But, same as in the horizontal direction, some other higher-order theories can be easily adapted to the axial direction in order to reduce diffusion errors.
The CHAPLET-3D(β-version) code, which employs the method introduced here, has been developed. The validation of the method has been performed by comparing the results of CHAPLET-3D calculations with those of multi-group Monte Carlo calculations in some 2-D and 3-D heterogeneous models. The results show that this 3-D calculation technique can give quite good accuracy for realistic cores (even axially solved by diffusion theory) and will makes it possible to solve large-scale 3-D heterogeneous core problems in deterministic methods by the present computer power.

Key Words: 3-D heterogeneous core calculation, 2-D MOC correction, non-linear iteration

1. INTRODUCTION

By virtue of recent improvement of computer performance, explicit geometry 2-D whole core problems has been enabled to be solved by deterministic transport methods, especially by the method of characteristics(MOC) [1]-[3]. But the direct extension to 3-D MOC whole core calculation is still difficult to be performed from the viewpoint of computer memory size and present CPU power.
As the intermediate idea between 2-D and 3-D MOC whole core calculations, the fusion technique of 2-D radial MOC calculation and 1-D axial calculation (by any methods) is thought to be a practical method to solve 3-D heterogeneous problems [4].

On the other hand, recently, the non-linear iteration technique[5], which is commonly used in the advanced nodal codes[5],[6], was adapted to accelerate 2-D MOC calculation and it made a great success to reduce the computational time dramatically[3],[7]. In this acceleration method, it is shown that the 2-D MOC solution can be reproduced by finite-difference form diffusion-like equations with additional non-linear coefficients obtained by the MOC calculation.
Applying this reproducibility, in this paper, 3-D heterogeneous core calculation, which is horizontally corrected by 2-D MOC solution utilizing non-linear iteration technique and axially solved by diffusion theory, has been achieved and verified its applicability.

2. METHODOLOGY

The 3-D analysis method described in this paper is based on the 3-D finite-difference(FDM) form diffusion–like calculation applying the non-linear iteration technique. At first, the basic FDM methodology is described. Then, the non-linear iteration technique and the method for 3-D core analysis with 2-D MOC correction are introduced in this section.

2.1. Finite-Difference Diffusion Calculation

In the usual FDM calculations, the neutron balance equation of a cubic cell is written by

$$-\underset{i=1,6}{Sum} J_i^g S_i + \Sigma_r^g \overline{\Phi}^g V = \overline{Q}^g V \,, \tag{1}$$

$$\overline{Q}^g = \frac{c^g}{Keff} \underset{g'}{Sumn} \Sigma_f^{g'} \overline{\Phi}^{g'} + \underset{g' \neq g}{Sum} \Sigma_s^{g' \to g} \overline{\Phi}^{g'} \,. \tag{2}$$

where

i	: direction index (6 surfaces)
J	: neutron current (incoming direction to the cell is positive direction)
S	: surface area
V	: volume of a cell
Σ_x	: macroscopic cross sections
$\overline{\Phi}$	: neutron scalar flux
g	: neutron energy group index (omitted after here).

The neutron current between adjacent two cells is estimated by

$$J_i = -D_i^{FDM} (\overline{\Phi} - \overline{\Phi}_I) \,, \tag{3}$$

$$D_i^{FDM} = 2D_I D / (Ddx_I + D_I dx) \tag{4}$$

where

I : adjacent cell index corresponding to the direction index i
D^{FDM} : FDM coefficient
D : diffusion coefficient ($=1/3\Sigma_{tr}$)
dx : cell width along the direction i

Substituting eq.(3) to eq.(1), the scalar flux of the center cell can be obtained by the average fluxes of 6 surrounding cells and updated by the next equation iteratively while it converges.

$$\overline{\Phi} = (\overline{Q}V + \underset{i=1,6}{Sum} D_i^{FDM} S_i \overline{\Phi}_I) / (\underset{i=1,6}{Sum} D_i^{FDM} S_i + \Sigma_r V) \tag{5}$$

2.2. Non-linear Iteration Technique

On the other hand, in the advanced nodal diffusion codes, the non-linear iteration techniques are commonly used to accelerate higher-order theory (e.g. nodal expansion model;NEM) models with lower-order diffusion models by introducing an additional diffusion-like coefficients as eq.(6). (cf. eq.3)

$$J_i = -D_i^{FDM} (\overline{\Phi} - \overline{\Phi}_I) - \widetilde{D}_i^{NEM} (\overline{\Phi} + \overline{\Phi}_I) \tag{6}$$

where

$\widetilde{D}^{NEM}$: NEM coefficient

Here, $\widetilde{D}^{NEM}$ s are obtained from the currents evaluated by the NEM theories.

$$\widetilde{D}^{NEM} = \left\{ -\widetilde{J}_i^{NEM} - D_i^{FDM} (\overline{\Phi} - \overline{\Phi}_I) \right\} / (\overline{\Phi} + \overline{\Phi}_I) \tag{7}$$

Substituting eq.(7) to eq.(1), the scalar flux considering NEM correction can be obtained similarly as eq.(5).

$$\overline{\Phi} = \left(\overline{Q}V + \underset{i=1,6}{Sum} (D_i^{FDM} - \widetilde{D}_i^{NEM}) S_i \overline{\Phi}_I \right) / \left(\underset{i=1,6}{Sum} (D_i^{FDM} + \widetilde{D}_i^{NEM}) S_i + \Sigma_r V \right) \tag{8}$$

In the same manner, this technique can also be applied to MOC calculations. In the references[3],[7], this application is utilized to accelerate 2-D MOC calculations.

$$J_i = -D_i^{FDM} (\overline{\Phi} - \overline{\Phi}_I) - \widetilde{D}_i^{MOC} (\overline{\Phi} + \overline{\Phi}_I) \tag{9}$$

2.3. 3-D Calculation with 2-D MOC Transport Corrections and 1-D Diffusion Solutions by Non-linear Iteration Technique

To achieve 3-D analysis with 2-D MOC transport corrections and 1-D diffusion solutions, the non-linear iteration technique is very useful to combine these two different theories. In the method of the advanced nodal diffusion analysis with the non-linear iteration technique (cf.eq.(8)), 2-D MOC transport corrections can be considered just by replacing the additional non-linear terms from the usual $\tilde{D}^{NEM}$ to $\tilde{D}^{MOC}$ in the horizontal directions. Then, eq.(8) is now modified as eq.(10).

$$\bar{\Phi} = \frac{\bar{Q}V + \underset{i=1,4}{Sum}(D_i^{FDM} - \tilde{D}_i^{MOC})S_i\bar{\Phi}_I + \underset{i=5,6}{Sum}(D_i^{FDM} - \tilde{D}_i^{NEM})S_i\bar{\Phi}_I}{\underset{i=1,4}{Sum}(D_i^{FDM} + \tilde{D}_i^{MOC})S_i + \underset{i=5,6}{Sum}(D_i^{FDM} + \tilde{D}_i^{NEM})S_i + \Sigma_r V} \tag{10}$$

where

i : 1-4=x-y plane, 5,6=z direction.

The 3-D calculation method introduced here can be described in the next flow chart.

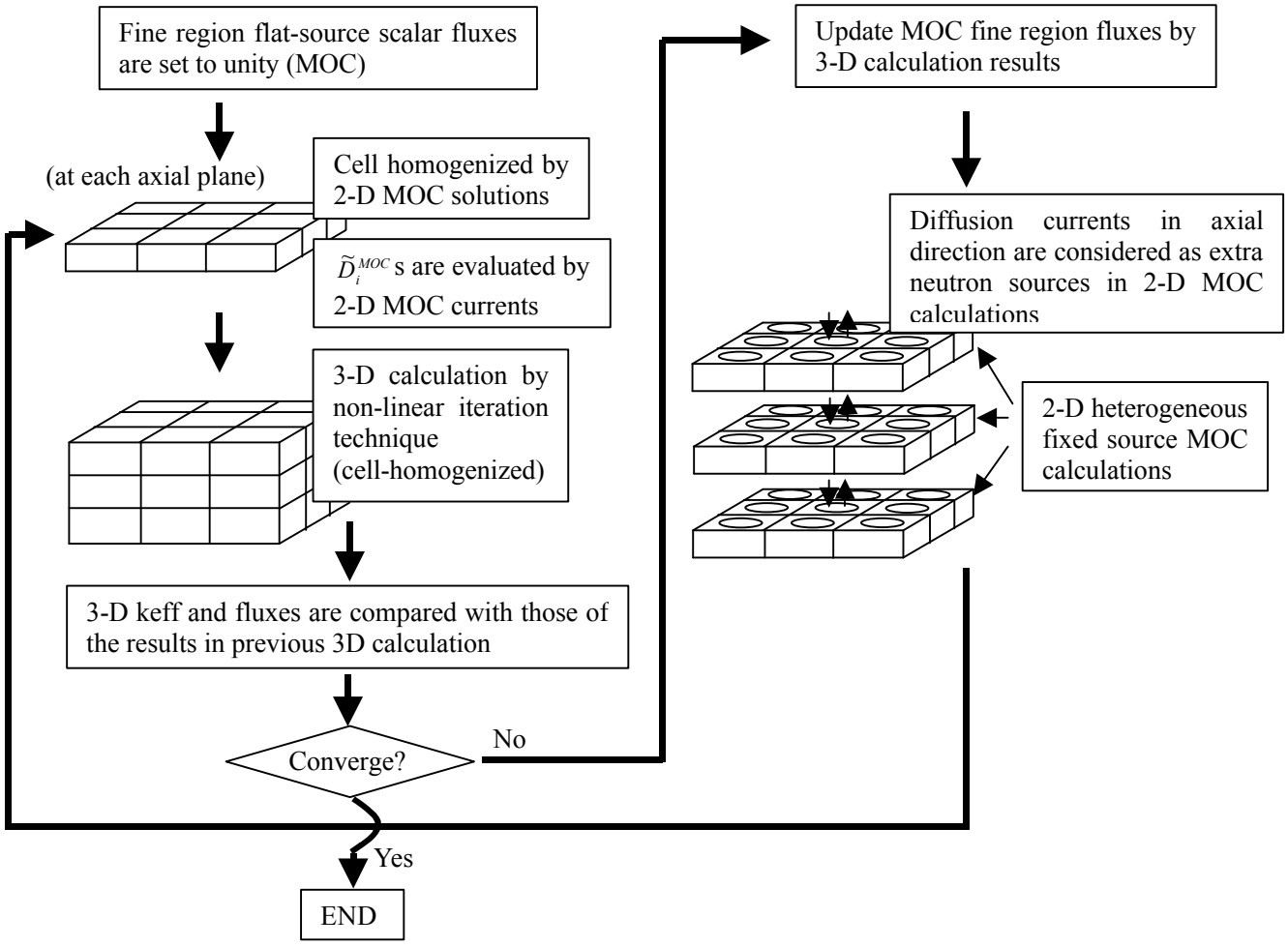

Figure 1 Calculation flow of 3-D core analysis with 2-D MOC corrections.

In the 2-D MOC heterogeneous calculations, the axial neutron streaming of 3-D calculation has to be considered appropriately. In this method, the axial currents are considered as extra sources distributed equally to the fine MOC regions in each cell.

Then, the characteristics equation in 2-D geometry can be described as follows.

$$dN / ds + \Sigma_{tr} N = (Q_k^{MOC} + q_k^{MOC,ext}) / 4p \ , \tag{11}$$

$$Q_k^{MOC} = \frac{c}{Keff} \underset{g'}{Sum} n\Sigma_f f_k + \underset{g'}{Sum} \Sigma_s f_k \, , \tag{12}$$

$$q_k^{MOC,ext} = (J_5 S_5 + J_6 S_6) / V_I \quad (k \in I) \, . \tag{13}$$

where

N: angular neutron flux
k: fine flat-source region index in MOC calculation
f : scalar flux of fine flat-source region in MOC calculation

Here, it should be noted that the consistency between Q_k^{MOC} and $q_k^{MOC,ext}$ must be taken. In other words, Q_k^{MOC} and $q_k^{MOC,ext}$ should be evaluated by the fluxes under the same normalization factor.
In the calculations presented later, 2-D MOC fine region fluxes are normalized by 3-D cell fluxes after each iterative 3-D calculation in order to take the consistency as eq.(14) and eq.(15). This normalization process also works as the acceleration of 2-D MOC calculations.

$$f_{k \in I}^{MOC,n+1} = \frac{\overline{\Phi}_I^{n+1}}{\overline{\Phi}_I^{n}} f_{k \in I}^{MOC,n} \tag{14}$$

$$\overline{\Phi}_I^{n} = \frac{\underset{k \in I}{Sum} f_k^{MOC,n} V_k}{V_I} \, , \quad (V_I = \underset{k \in I}{Sum} V_k) \tag{15}$$

These 2-D MOC calculations are solved as fixed-source problems. Consequently, the main 3-D solution and 2-D MOC calculations are converging synchronously.

2.4 Code Development

A 3-D core analysis code CHAPLET-3D, which employs the method presented here, has been developed. In this code, to reduce memory size, the neutron tracking paths used for 2-D MOC calculations are commonly shared to the axial planes which have same geometry.
Some main features and restrictions of the code are described below.

- Main 3-D calculation
  - Core configuration is constructed from XYZ rectangular parallelepiped grid cell (in those cells, any 2-D geometry can be defined.)
  - FDM or NEM diffusion method can be chosen for the axial solver
- 2-D MOC calculation
  - Isotropic scattering is assumed
  - Exact geometry can be treated

3. VERIFICATION TESTS

To validate this calculation method, some sample tests have been performed by CHAPLET-3D code in both 2-D and 3-D geometries. In this series of the verification, the reference solutions were obtained from GMVP (multi-group Monte Carlo) code[8]. In the reference Monte Carlo calculations, the cross sections and geometries used are identical with those of CHAPLET-3D calculations. These test calculations were performed in 7 energy groups.

3.1. Two Dimensional Tests

To confirm the accuracy of MOC calculations, 2-D model analyses were performed. Correctly, it confirms the reproducibility of the non-linear iteration technique applying to 2-D MOC calculations.

Figure 2 shows the models used for 2-D verification tests.

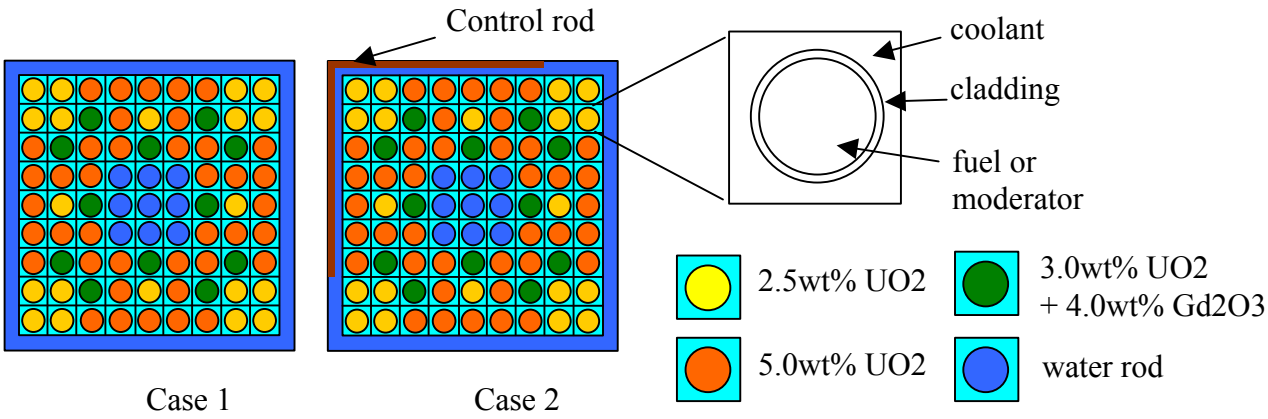

Figure 2 Calculation models for 2-D verification tests

In the 2-D MOC calculation, the coolant region is divided into 48 fine flat-source regions (3 cylindrically x 16 azimuthally). The fuel and cladding is divided into 16 regions azimuthally. About the discretization parameter of the tracking paths in the MOC calculations, the number of azimuthal angle is 64, tracking width is 0.5mm and the number of polar angle is 2[9]. As for the reference GMVP calculations, the number of the effective neutron history was 1,000,000 (total 1,200,000 his.). The statistical error of the pin power is about 1%.

The results for the pin power distributions and the effective multiplication factors(k_{eff}) are shown in the next figure.

(CASE 1: CR-withdrawn)

1.200	0.985	1.454	1.385	1.384	1.385	1.454	0.985	1.200
0.985	0.739	0.344	1.067	0.621	1.067	0.344	0.739	0.985
1.454	0.344	0.981	1.126	0.351	1.126	0.981	0.344	1.454
1.385	1.067	1.126	0.000	0.000	0.000	1.126	1.067	1.385
1.384	0.621	0.351	0.000	0.000	0.000	0.351	0.621	1.384
1.385	1.067	1.126	0.000	0.000	0.000	1.126	1.067	1.385
1.454	0.344	0.981	1.126	0.351	1.126	0.981	0.344	1.454
0.985	0.739	0.344	1.067	0.621	1.067	0.344	0.739	0.985
1.200	0.985	1.454	1.385	1.384	1.385	1.454	0.985	1.200

Pin power distribution of CHAPLET-3D.

-0.7	-0.4	0.4	-0.9	0.2	-0.3	-0.5	-0.3	-1.7
0.1	-0.5	-0.1	0.0	-0.1	0.9	-0.1	-0.2	-0.8
-0.5	-0.2	0.1	1.1	-0.2	0.4	0.4	-0.2	-0.4
-0.7	-0.1	-0.2	0.0	0.0	0.0	0.6	0.0	0.3
-0.5	0.2	0.2	0.0	0.0	0.0	-0.2	0.1	-0.1
-0.6	-0.6	-0.3	0.0	0.0	0.0	-0.6	0.2	0.0
0.2	0.1	0.9	0.3	-0.1	0.2	-0.3	0.1	0.4
0.1	0.2	0.0	1.7	-0.1	0.6	-0.1	0.0	-0.4
-0.2	-0.2	0.3	0.4	1.7	0.9	-0.1	0.4	-0.1

% errors vs GMVP (RMS:0.53%)

(CASE 2: CR-inserted)

0.216	0.258	0.470	0.553	0.626	0.707	0.943	0.909	1.299
0.258	0.304	0.256	0.739	0.469	0.881	0.365	0.791	1.134
0.470	0.256	0.806	1.046	0.374	1.207	1.122	0.432	1.797
0.553	0.739	1.046	0.000	0.000	0.000	1.387	1.380	1.821
0.626	0.469	0.374	0.000	0.000	0.000	0.469	0.843	1.899
0.707	0.881	1.207	0.000	0.000	0.000	1.516	1.486	1.964
0.943	0.365	1.122	1.387	0.469	1.516	1.365	0.504	2.115
0.909	0.791	0.432	1.380	0.843	1.486	0.504	1.088	1.457
1.299	1.134	1.797	1.821	1.899	1.964	2.115	1.457	1.786

Pin power distribution of CHAPLET-3D.

0.0	0.0	0.0	-0.8	0.0	-0.8	-0.3	-0.4	-0.7
-0.2	0.0	0.0	-0.5	0.4	0.6	0.0	-0.5	-0.4
-0.2	0.1	-0.9	0.7	-0.1	-1.1	0.5	-0.1	0.6
0.1	-0.5	0.0	0.0	0.0	0.0	-0.4	0.2	0.2
-0.4	0.0	-0.2	0.0	0.0	0.0	-0.1	0.2	0.2
0.6	-0.4	-0.5	0.0	0.0	0.0	-0.5	0.6	1.0
1.1	-0.2	-0.5	-0.1	0.0	-0.3	0.1	0.1	0.4
-1.0	-0.4	-0.2	-0.5	0.3	0.3	0.2	0.3	0.6
-1.0	0.1	0.4	0.0	0.0	0.7	1.2	-0.5	-0.2

% errors vs GMVP (RMS:0.49%)

Numerical results for the effective multiplication factor

	GMVP	CHAPLET-3D	Error
CASE 1	1.0188 (± 0.039%)*1	1.0191	+0.03%dk
CASE 2	0.7905 (± 0.056%)	0.7902	- 0.03%dk

*1:Standard deviation

Figure 3 The results of 2-D verification tests

As shown in Figure 3, the results of 2-D CHAPLET-3D calculations agree very well with the reference Monte Carlo results within the statistical errors.

3.2. Three Dimensional Tests

After confirming the accuracy of 2-D calculation, the validity of 3-D CHAPLET-3D calculation has been verified.

Figure 4 shows the 3-D test configuration used for this verification. Two core conditions, one is CR-withdrawn(case 3) and the other is CR partially inserted(case4), were analyzed.

In the CHAPLET-3D calculations, some different axial treatments were examined.(see Table I) In the reference GMVP calculations for these 3-D cases, the number of the effective neutron history was set to10,000,000 (total 15,000,000 his.).

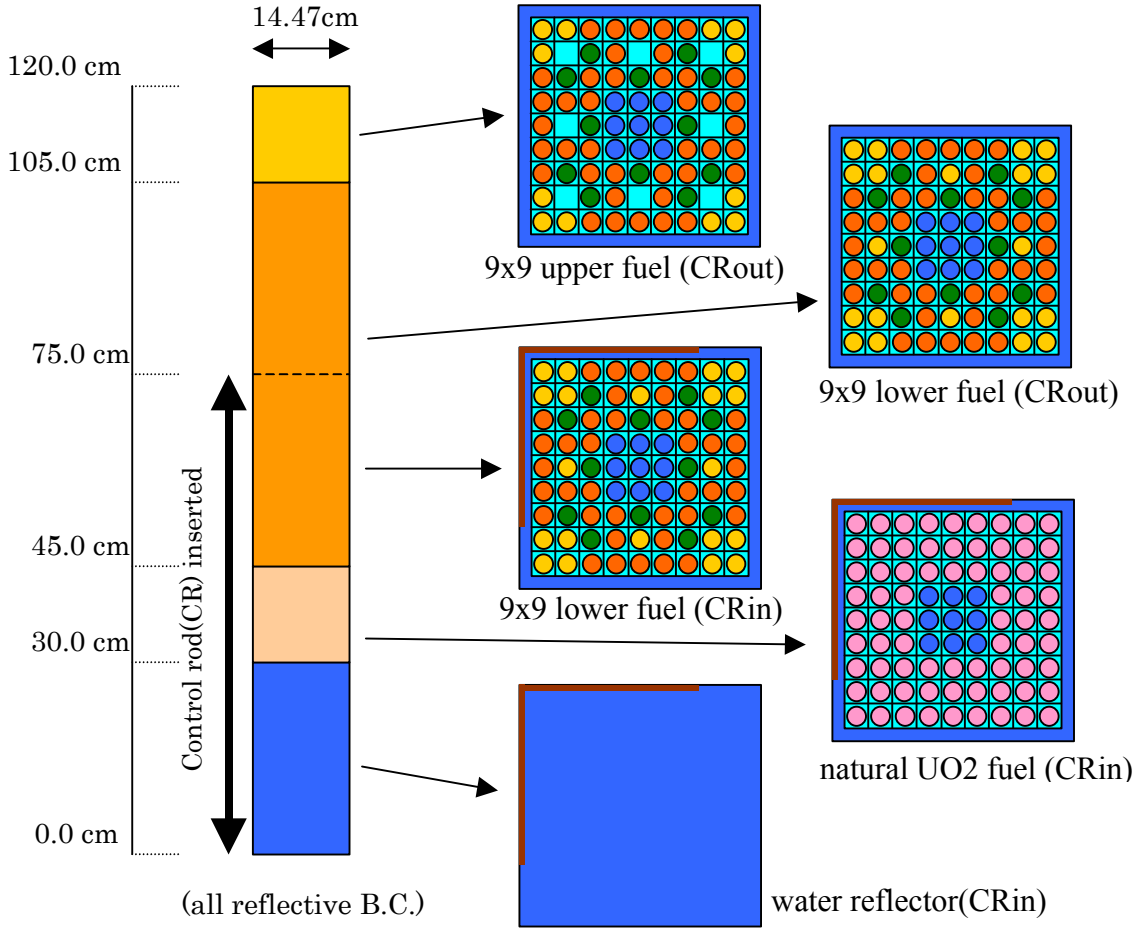

Figure 4 Calculation model for 3-D verification tests (CR-inserted case)

Table I Axial treatments in 3-D CHAPLET-3D calculations

	Axial treatment	Axial pitch
Method 1	FDM diffusion	15cm (8 planes)
Method 2	NEM diffusion	15cm (8 planes)
Method 3	FDM diffusion	3cm (40 planes)
Method 4	NEM diffusion	3cm (40 planes)

Table II and Table III show the results for the effective multiplication factor and the axial/pin power distributions in case 3 and 4, respectively.

As for the case 3, the CR-withdrawn case, the results are fairly good independently of the axial meshing. The multiplication factors and the axial power distributions agree within 0.1%dk and 1.5%, respectively. On the contrary, for the case of CR-inserted (case 4), the errors became large in rough axial meshing calculations(method1,2). It shows that the rapid 2-D flux shape change (from a higher-mode to the fundamental mode) due to localized axial currents can't be followed by too thick 2-D MOC calculations, because the infinite axial structure is assumed in each 2-D MOC calculation. In the cases of fine axial meshing analyses (method3,4), however, these large errors are disappeared and the RMS errors of pin power are almost same as those of 2-D test results. (cf. Figure 3)

Table II Verification results of CASE 3 (CR-withdrawn)

	GMVP	Method 1	Method 2	Method 3	Method 4
k_{eff}	0.9990 (±0.02%)	+0.08%dk	+0.06%dk	+0.03%dk	+0.03%dk
axial zones	axial power dist.	axial power errors (%)			
zone6 (z=105-120)	1.474 (±0.64%)	-1.3%[*1]	-1.5%	0.1%	0.1%
zone5 (z=90-105)	1.422 (±0.67%)	-1.1%	-0.5%	-0.5%	-0.3%
zone4 (z=75-90)	1.254 (±0.71%)	0.4%	0.4%	-0.1%	-0.1%
zone3 (z=60-75)	0.990 (±0.80%)	1.3%	0.7%	0.0%	-0.0%
zone2 (z=45-60)	0.669 (±0.97%)	0.1%	0.7%	-0.3%	-0.2%
zone1 (z=30-45)	0.192 (±0.95%)	0.6%	0.3%	0.7%	0.4%
pin power err.[*2]	-	0.82%	0.68%	0.49%	0.41%

***1: %errors in axial zone power (CHAPLET-Ref.)**
***2: %RMS errors in pin power normalized by (72pins x 6 axial zones)**

Table III Verification results of CASE 4 (CR-inserted)

	GMVP	Method 1	Method 2	Method 3	Method 4
k_{eff}	0.9762(±0.02%)	+0.33%dk	+0.34%dk	+0.05%dk	+0.02%dk
axial zones	axial power dist.	axial power errors (%)			
zone6 (z=105-120)	2.207 (±0.49%)	-4.4%	-4.0%	-1.4%	-0.8%
zone5 (z=90-105)	1.904 (±0.54%)	-0.8%	0.5%	-1.2%	-0.7%
zone4 (z=75-90)	1.243 (±0.66%)	8.1%	7.8%	1.4%	0.8%
zone3 (z=60-75)	0.448 (±1.07%)	-2.3%	-3.3%	0.8%	0.5%
zone2 (z=45-60)	0.168 (±1.76%)	-0.5%	-1.0%	0.2%	0.2%
zone1 (z=30-45)	0.029 (±2.19%)	0.1%	0.0%	0.1%	0.1%
pin power err.	-	2.87%	3.00%	0.78%	0.51%

Figure 5 and Figure 6 show the number of outer(MOC) iterations and CPU(intel 2GHz) time in CHAPLET-3D calculations, respectively. By grace of the acceleration effects of the non-linear iteration, 2-D MOC calculations are converged in very small number of iterations. Of course, in each outer iteration, usually 3-50 times 3-D FDM like outer iteration are required inside. As far as in these test cases, the CPU time is almost proportional to the number of axial planes.
The required memory size was about 30MB in 2-D case and was150MB in the method 4 of the case 4.

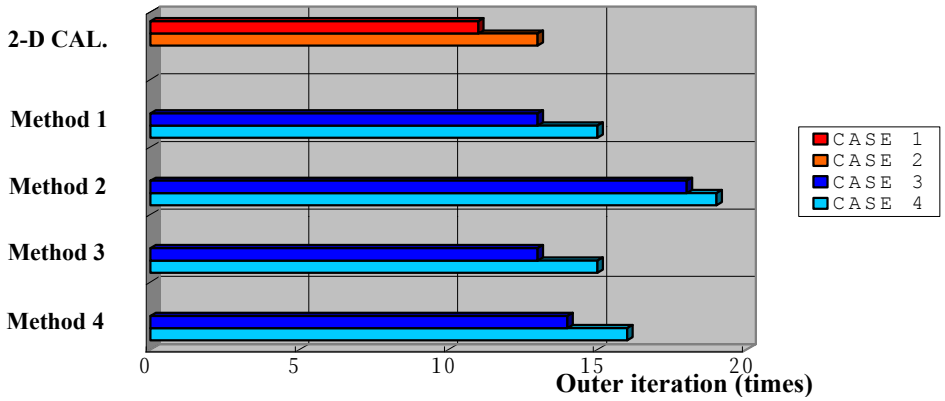

Figure 5 The number of outer iterations in CHAPLET-3D calculations

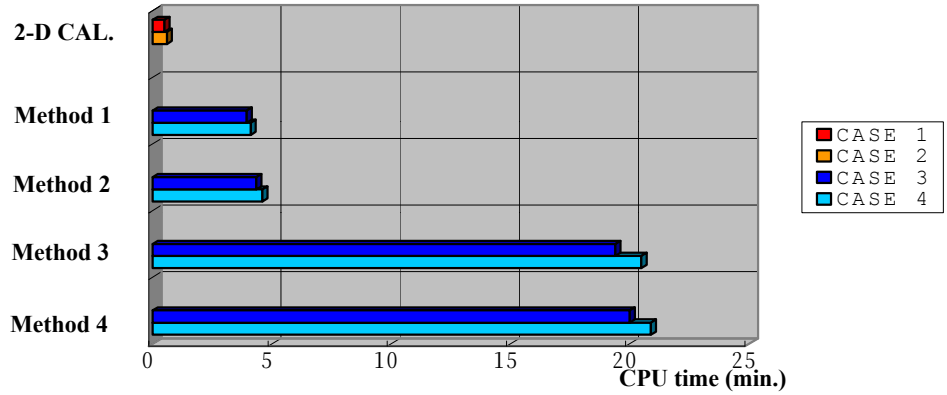

Figure 6 CPU time of CHAPLET-3D calculations

4. DISCUSSION

- As reported in the reference [7], the direct use of $\tilde{D}^{MOC}$ to the non-linear iteration may cause divergence problem. Actually, some CHAPLET-3D calculations presented here required proper relaxation procedures. Especially, the cases which have large reflector regions, large strong absorber regions or void cells may not converge or need some efforts to

converge.

- To obtain $\tilde{J}_i^{MOC}$, required for evaluating $\tilde{D}^{MOC}$, accumulation of the net-current needed in the MOC transport sweep. This process may be the most important part for quick calculation and smooth convergence. If the net-currents and related cell fluxes are not consistent between 2-D MOC and 3-D calculations, it doesn't converge or may lead false-convergence (but usually small error observed).
- In this paper, each pin cell is considered as a node for the non-linear iteration. This grid might be changed to the assembly unit. But, in that case, the effect of MOC acceleration becomes small and the local axial streaming can't be treated.

5. CONCLUSIONS

The method for diffusion-like 3-D heterogeneous core calculations, which is corrected by 2-D MOC solutions horizontally and solved by the diffusion theory axially, has been introduced and validated. In this method, the non-linear iteration technique is utilized to consider 2-D MOC transport corrections for usual 3-D diffusion nodal analysis. Fortunately, because of its simplicity, this method is easy to apply to the conventional nodal codes.

The 3-D results of CHAPLET-3D code are remarkably accurate, even the diffusion theory is employed for the axial solver, and show that this method presented here could be one prospective calculational technique for solving 3-D large-scale heterogeneous core problems by deterministic methods with realistic computer resources.

REFERENCES

1. S.Kosaka and E.Saji, "Transport Theory Calculation for a Heterogeneous Multi-Assembly Problem by Characteristics Method with Direct Neutron Path Linking Technique," *Journal of Nuclear Science and Technology*, **Vol.37**, No.12, p1015 (2000)
2. N.Z.Cho, et al., "Whole-Core Heterogeneous Transport Calculations and Their Comparisons with Diffusion Results," *Trans. Am. Nucl. Soc.,* **Vol.83**, p292 (2000)
3. K.S.Smith and J.D.Rhodes, "CASMO-4 Characteristics Method for Two-Dimensional PWR and BWR Core Calculations," *Trans. Am. Nucl. Soc.,* **Vol.83**, p294 (2000)
4. N.Z.Cho, et al., "Fusion of Method of Characteristics and Nodal Method for 3-D Whole-Core Transport Calculation," *Trans. Am. Nucl. Soc.,* **Vol.86**, p322 (2002)
5. K.S.Smith, "Nodal Method Storage Reduction by Nonlinear Iteration," *Trans. Am. Nucl. Soc.,* **Vol.44**, p265 (1984)
6. C.Lee and T.J.Downar, "Nonlinear Formulation for Multigroup Simplified P3," *Trans. Am. Nucl. Soc.,* **Vol.83**, p297 (2000)
7. K.S.Smith and J.D.Rhodes, "Full-Core,2-D, LWR Core Calculations with CASMO-4E," *Proc. PHYSOR2002*, Seoul, Korea, October 7-10, 2002 (CD-ROM)
8. T.Mori and M.Nakagawa, JAERI-Data/Code 94-007 (1994)
9. A.Leonard and C.T.McDaniel, "Optimal Polar Angles and Weights for the Characteristics Method," *Trans. Am. Nucl. Soc*., **Vol.73**, p172 (1995)